The Astrophysical Journal, 738:133 (6pp), 2011 September 10 doi:10.1088/0004-637X/738/2/133

HDO INFRARED DETECTION SENSITIVITY AND D/H ISOTOPIC EXCHANGE IN AMORPHOUS AND CRYSTALLINE ICE

Óscar Gálvez, Belén Maté, Víctor J. Herrero, and Rafael Escribano
Instituto de Estructura de la Materia, IEM-CSIC, Serrano 123, 28006 Madrid, Spain
Received 2011 June 27; accepted 2011 June 27; published 2011 August 18

ABSTRACT

The sensitivity of the OD stretching band as a probe to detect HDO in astrophysical ice is discussed based on IR laboratory spectra of HDO molecules embedded in H_2O ice. This band is extremely broad and tends to disappear into the absorption continuum of H_2O for low-temperature amorphous samples. Detectable HDO/H_2O ratios with this technique may range from a few percent for amorphous samples to a few per thousand in crystalline ice. These relatively high upper limits and the appreciable dependence of the band shape on temperature, which would complicate the interpretation of data from many lines of sight, decisively limit the usefulness of the technique for HDO detection in astronomical observations. The process of isotopic H/D exchange in mixed ice of H_2O/D_2O is also studied through the evolution of the OD band in IR spectra. Isotopic exchange starts at ∼120 K and is greatly accelerated at 150 K, as crystallization proceeds in the ice. Annealed amorphous samples prove to be more favorable for isotope exchange than samples directly formed in crystalline phase. The annealing process seems to favor a polycrystalline ice morphology with a higher defect activity. These morphology differences can be of relevance for deuterium fractionation in astronomical environments.

Key words: infrared: general – methods: laboratory – molecular processes – techniques: spectroscopic

Online-only material: color figures

1. INTRODUCTION

Molecular isotopic distributions hold valuable clues for understanding the properties and evolution of astronomical environments. Appreciable deuterium fractionation is found in cold clouds (see for instance Turner 2001), where it is believed to be caused by zero-point energy effects associated with ion–molecule chemistry (Millar 2005), but extreme deuterium enrichment with the presence of polydeuterated species has also been found in low-mass protostellar cores (Loinard et al. 2002; Parise et al. 2004; Ceccarelli et al. 2007), where many of the available molecules evaporate from ice mantels. Although it is assumed that the observed D enrichment is caused to a great extent by species generated in the gas phase and accreted on the grains in colder phases of star evolution, it is now generally accepted that chemical reactions on or in the grain mantels must also be considered to get the complete fractionation picture (Tielens 1983; Rodgers & Millar 1996; Roberts et al. 2002).

Among D bearing molecules, water is especially interesting from many points of view. In particular the HOD/H_2O ratio is crucial in studies about the formation of the solar system and the Earth (Robert et al. 2000; Robert 2001). With respect to other hydrogen containing molecules, the D enrichment observed in water is relatively small. Attempts to measure directly the HOD/H_2O ratio in the ice, based on IR measurements, provided upper limits in the range from 0.002 to 0.02 in protostar samples (Dartois et al. 2003; Parise et al. 2003). These values are not too stringent and reveal probably the relative insensitivity of the IR method. Measurements of the gas-phase HDO/H_2O ratio in protostellar regions using more sensitive millimetric techniques have provided lower values which range from 0.03 (Parise et al 2005) to $\sim(3–6) \times 10^{-4}$ (Stark et al. 2004; Jørgensen & van Dishoeck 2010), the latter being more in line with the magnitude of the HDO/H_2O quotient measured in comets (3–4) $\times 10^{-4}$ (Bockelée-Morvan 1998; Villanueva et al. 2009) and in Earth's oceans $\sim 1.5 \times 10^{-4}$ (Robert 2001). However, recent observations of the low-mass protostar NGC1333-IRAS2A reveal an HDO/H_2O abundance ratio greater than 1% (Liu et al. 2011).

Much higher D enrichments have been observed in other species like methanol, for which ratios of deuterated to non-deuterated molecules as high as 0.4 have been reported (Parise et al. 2004). Solid phase deuteration mechanisms through successive atomic addition or, more likely, through D/H substitution in previously formed CH_3OH, have been demonstrated in laboratory experiments (Watanabe & Kouchi 2008). The deuteration was found to happen almost exclusively at the methyl group, which is consistent with the very low gas phase CH_3OD/CH_2DOH ratios detected in protostellar sources (Parise et al. 2004).

A complementary explanation for the low gas phase relative concentration of CH_3OD has been recently provided by Ratajczak et al. (2009), who showed that the D atoms in the hydroxylic groups of methanol are efficiently exchanged with H atoms from the ice network at $T > 120$ K. This preferential loss of D should not be restricted to methanol, but would also take place in other molecules possessing a hydroxilic group. The H/D exchange in ice has been studied by various groups with different experimental techniques (see for instance Devlin 1990; Lee et al. 2006; Geil et al. 2005; Devlin & Buch 2007, and references therein) and although some aspects of the detailed mechanism are still controversial, it has been established that it is mainly driven by proton (or deuteron) transfer assisted by the propagation of orientational defects.

In astronomical environments, different processes of compaction, amorphization, and crystallization caused by radiation, impacts of solid bodies, or thermal processing are expected to lead to a wide variety of ice (Kouchi & Yamamoto 1995; Baragiola 2003; Palumbo 2005; Raut et al. 2008), which could exhibit different propensities for D/H exchange and could thus have an influence on the observed molecular deuterium fractionation. The temperature for the start of efficient D/H

exchange corresponds roughly to the transition from amorphous to crystalline ice that takes place as part of the evolution of protostellar cores and also in many solar system objects, and it is conceivable that the morphology of the initial amorphous ice could influence the defect mobility of the crystalline ice produced from it.

In this work, we present an IR investigation of D/H exchange in ice samples with different structure and morphology. This technique has been validated since the 1980s by Devlin and coworkers (Collier et al. 1984; Devlin 1990) and we take here advantage of their spectroscopic characterization of the OD vibration bands in ice. We have investigated D/H exchange in amorphous and crystalline vapor deposited samples of H_2O with small amounts of D_2O as a function of temperature (between 14 and 150 K) and D_2O proportion (from 0.4% to 10%). Similarities and differences in the efficiency of isotopic exchange between the various samples are discussed. Experiments carried out directly on amorphous and crystalline samples of water ice containing variable amounts of HDO allow also an approximate assessment of the upper limit estimates for the proportion of D in water ice attainable with IR measurements.

2. EXPERIMENTAL

The experimental setup has been described in detail elsewhere (Gálvez et al. 2008; Maté et al. 2003; Carrasco et al. 2002). It consists of a closed cycle helium cryostat with a cold finger in close contact with a Si plate onto which our gas mixtures are condensed. The temperature of the substrate can be controlled between 14 K and 300 K with an accuracy of 1 K. The system is located in a high vacuum chamber with a background pressure of 10^{-8} mbar that is coupled through a purged pathway to a Vertex70 Bruker FTIR spectrometer. The spectra presented here were recorded at resolution of 2 cm^{-1} using a liquid-nitrogen cooled mercury cadmium telluride (MCT) detector and accumulating 500 scans.

Ice films of HDO/H_2O mixtures were generated on the substrate at 14 K by deposition of vapor from room temperature solutions of HDO in H_2O. The HDO/H_2O liquid solutions were in turn prepared by diluting D_2O in volume proportions of 0.4%, 2%, and 10% in H_2O. Isotopic scrambling transforms then virtually all D_2O molecules into HDO and leads to equilibrium concentrations of 0.8%, 4%, and 20% of HDO in water (the most concentrated mixture contained also an amount of D_2O as estimated from an IR spectrum of the liquid to be less than 1%). Given the relatively small mass differences between H_2O and HDO no significant separation of the two isotopic species is expected during deposition and we have assumed that the solid films have the same HDO/H_2O ratios as the liquid solutions.

Ice layers of H_2O/D_2O mixtures were produced by introducing simultaneously H_2O and D_2O vapors through independent lines to backfill the chamber. The partial pressures were varied between 7×10^{-6} and 1.3×10^{-5} mbar for H_2O, and between 5×10^{-8} and 8×10^{-7} mbar for D_2O. After several minutes of deposition, films with a thickness of ~300 nm were obtained. Water pressures were determined from the growing rates of pure water ice films deposited at 150 K via the integrated band strength of the 3200 cm^{-1} OH stretch band of water at that temperature, $A = 2.7 \times 10^{-16}$ cm $molecule^{-1}$, taken from Mastrapa et al. (2009). D_2O measurements were based on the 2450 cm^{-1} band of D_2O in pure D_2O ice films deposited at 150 K, for which an integrated band strength value was used of $A = 1.4 \times 10^{-16}$ cm $molecule^{-1}$, calculated by scaling the OH band strength given above with a factor of $A(D_2O)/A(H_2O) =$ 0.518, as reported by Ikawa & Maeda (1968). The described procedure for the estimation of the vapor partial pressures was checked repeatedly and was found to be very reliable, its linearity extending over an approximate three orders of magnitude range, which allowed the preparation of ice samples with a high D_2O dilution. In this work ice mixtures with D_2O/H_2O proportions of $0.4\% \pm 0.1\%$, $3\% \pm 0.3\%$, and $10\% \pm 1\%$ were generated at 14 K, 90 K, and 150 K.

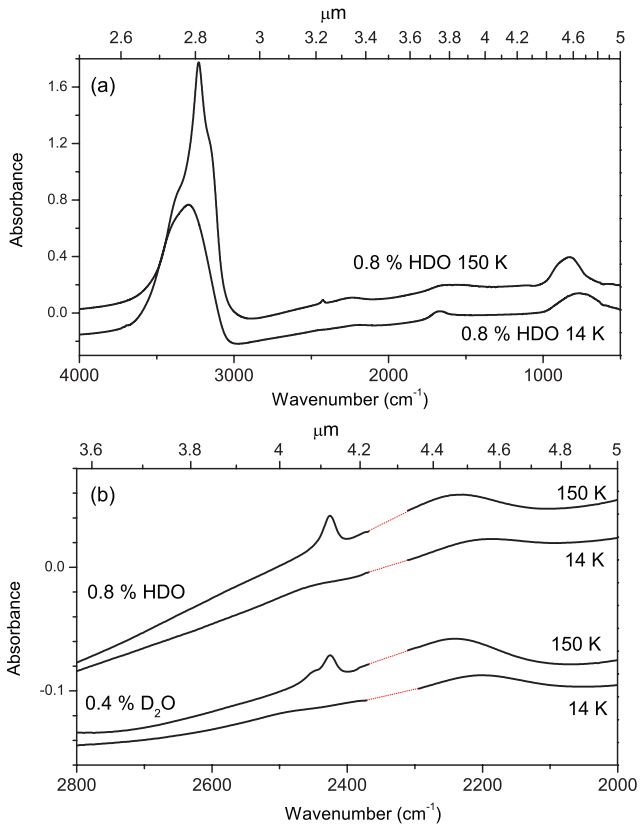

Figure 1. (a) Mid-infrared spectra of a 0.8% mixture of HDO in H_2O ice as deposited at 14 K and after heating the sample to 150 K. (b) Infrared spectra of the OD stretching region of two vapor deposited ice mixtures as generated at 14 K and after several minutes at 150 K. The two upper traces correspond to a HDO/H_2O ice mixture with HDO concentration of 0.8% and the two lower traces to a D_2O/H_2O ice mixture with a D_2O concentration of 0.4%. The curve intervals marked with red dots indicate the position of the intense stretching mode of ambient CO_2 that cannot be properly removed.

(A color version of this figure is available in the online journal.)

To explore the conversion of D_2O to HDO in our diluted mixtures (0.4% D_2O molecular fraction) their time evolution at 150 K was followed. The samples grown at lower temperatures were heated to 150 K at 5 K $minute^{-1}$. The $n(HDO)/n(D_2O)$ ratio was determined from the relative intensity of the bands observed in the infrared spectra of our 150 K ice at ~2449 cm^{-1} and at ~2425 cm^{-1}, assigned to the OD antisymmetric stretching band of D_2O and to the OD stretching band of HDO, respectively. For these two bands we have taken the quotient of absorption coefficients proposed by Devlin and coworkers (Collier et al. 1984), $A(D_2O)/A(HDO) = 1.31$.

3. RESULTS AND DISCUSSION

The upper panel of Figure 1 displays the mid-IR spectrum of an H_2O/HDO ice sample with a 0.8% proportion of HDO deposited at 14 K, and the spectrum after heating the sample to 150 K and keeping it at this temperature for several minutes.

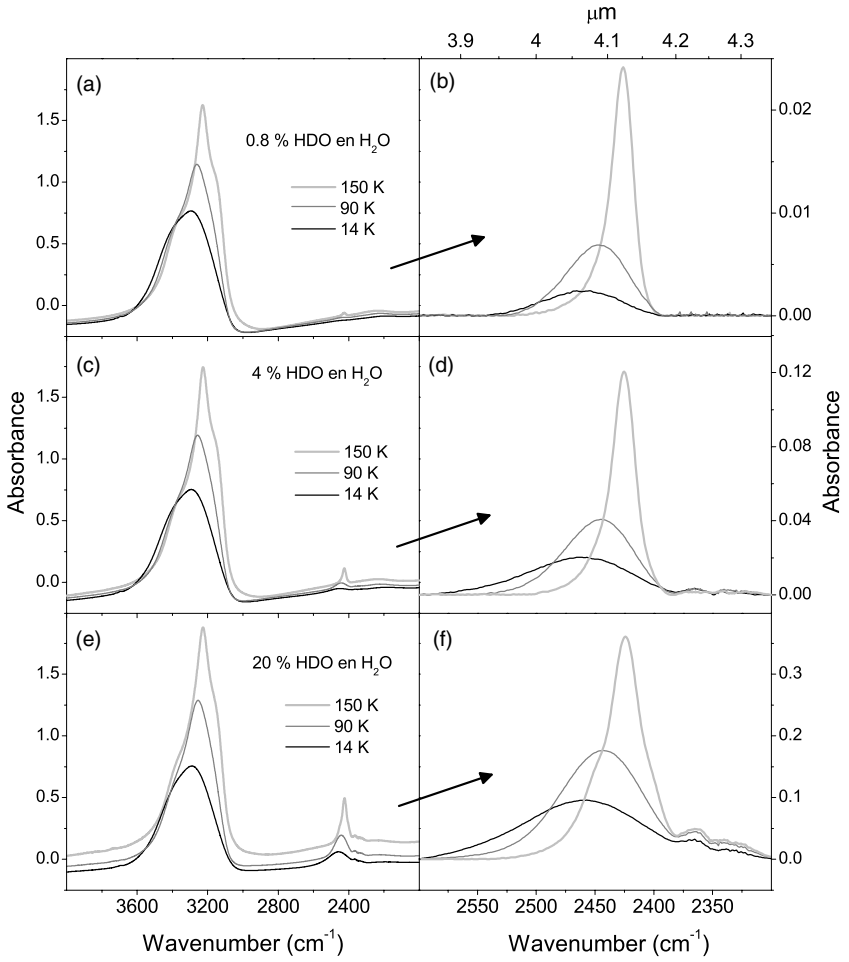

Figure 2. IR spectra of HDO:H_2O mixtures generated at 14 K and heated then to 90 K and to 150 K at 5 K minute^{-1}. The 150 K spectra were recorded after 20 minutes at that temperature. Left panels (a), (c), and (e) correspond to HDO mixture proportions of 0.8%, 4%, and 20%, respectively. The corresponding right panels show an enlargement of the OD stretching region.

The transition from an amorphous to a crystalline structure is clearly visible in the change of the OH stretch band shape at ∼3000–3600 cm^{-1}. The spectral interval between 2000 and 2800 cm^{-1} is amplified in the two upper traces of the lower panel. In the 14 K amorphous sample, a barely appreciable broadband, hardly distinguishable in the figure from the underlying absorption continuum, appears in the 2400–2600 cm^{-1} region, which is the frequency range of OD stretch vibrations. In contrast with the broad absorption of the amorphous film, a clear peak at ∼2425 cm^{-1} (4.1 μm) is visible in the 150 K spectrum of crystalline ice. This band narrowing with growing temperature is consistent with previous literature measurements (Mayer & Pletzer 1985; Hague et al 1994; Dartois et al. 2003) and was used by Hague et al. (1994) for the study of the crystallization kinetics of water in hyperquenched glassy samples below 150 K. It can be rationalized in terms of the distribution of nearest neighbor oxygen–oxygen distances that is very broad for the cold amorphous samples (Madden et al. 1978), but becomes much narrower with the decrease of local disorder induced by the temperature rise.

The HDO spectra are compared in the same panel with analogous measurements, for a H_2O/D_2O ice layer with a 0.4% concentration of D_2O (i.e. with the same D/H proportion). A hardly appreciable broadband comparable to that of the H_2O/HDO film is also found at 14 K, but in this case an overlapping two peak structure is revealed upon heating to 150 K. By analogy with the results of Collier et al. (1984), the higher frequency peak is assigned to the antisymmetric OD stretching mode of D_2O, and the lower frequency peak to the OD stretching of HDO, both isolated in a H_2O matrix. The gradual appearance of the HOD peak in the spectra, indicative of H/D exchange, starts at a temperature of ∼120 K, but the process accelerates significantly when the temperature approaches 150 K. Before looking more deeply at the H/D exchange, we will pause to consider in some detail the dependence of the OD stretching band of HDO on ice conditions.

Figure 2 shows spectra of ice layers with HOD/H_2O proportions of 0.8%, 4%, and 20%, deposited at 14 K and then heated to 90 and to 150 K. The 4000–2000 cm^{-1} wavenumber interval comprising the bands of both OH and OD stretch vibrations is presented in the left part of the figure (panels (a), (c), and (e)) and a blow up of the spectral region between 2300 and 2600 cm^{-1} (panels (b), (d), and (f)) provides an enlarged view of the weak OD bands. Using the measurements for the 4% HDO mixture and the integrated absorbances of Mastrapa et al. (2009) for the OH band of H_2O, we have derived the corresponding absorbances for the OD band of HDO at 150 K and at 14 K. At the higher temperature, corresponding to crystalline ice, we find $A_{OD}(150\ K) = (6.4 \pm 0.3) \times 10^{-17}$ cm molecule^{-1}. This value is ∼25% larger than that reported by Ikawa & Maeda (1968) and the difference reflects just the higher $A_{OH}(150\ K)$ from recent work of Mastrapa et al. (2009) that has been used

here as a reference. At 14 K we obtain $A_{OD}(14\ K) = (4.1 \pm 0.4) \times 10^{-17}$ cm molecule^{-1} in good accordance with the value proposed by Dartois et al. (2003). For the most diluted mixture (0.8% HDO) the $A_{OD}(150\ K)$ value is still coincident within 10% with that derived for the 4% HDO solution just commented on, but estimates for the 14 K sample are plagued by errors higher than 50% due mostly to the larger uncertainty in the baseline (see Figure 1). For more diluted HDO mixtures the band contour definition becomes gradually more problematic and concentration estimates turns unreliable.

The large width of the OD stretching band in the amorphous samples generated at very low temperature, which can bury weak signals into the absorption continuum, limits the sensitivity of the IR technique, for the detection of HDO. As the OD band narrows with growing temperature, an increase in detection sensitivity takes place. This increase in sensitivity starts already in the amorphous phase, as demonstrated by the 90 K spectra, and is maximal for the crystalline samples. We estimate that for diluted mixtures the detection sensitivity of HDO in crystalline ice is roughly an order of magnitude higher than that for the corresponding low-temperature amorphous solid. An inspection of the right part (panels (b), (d), and (f)) of Figure 2 shows that the relative intensities and widths of the OD bands for the three temperatures represented depend also on HDO/H_2O ratio. The simultaneous variability of the OD band with temperature and isotopic composition of the sample poses additional limitations for its use in astronomical observations.

A major practical constraint for the detection of HDO in astronomical ice is the interference from other species. Dartois et al. (2003) contested the previous assignment of small OD bands by Teixeira et al. (1999) in spectral data from the Infrared Space Observatory toward the protostar W33A and pointed out that for this and other sources the identification of OD bands from water would be impaired by the presence of solid methanol, which is a common constituent of ice mantels. For sources with a much smaller methanol content upper limits as low as 0.2%–0.5% (Dartois et al. 2003; Parise et al. 2003) have been reported for the HDO/H_2O ratio in samples with a large amount of crystalline ice. Our results suggest that these HDO fractions could be observable in pure crystalline ice, but in amorphous ice a proportion of HDO lower than 1% or, more likely a few percent, considering the uncertainties usually associated with the processing of observational data, would be undetectable. The frequency spreading of the OD stretch vibration renders this band too broad and unnoticeable, even in the absence of interferences from other molecules. This would make IR measurements useless for the estimate of HDO in the ice mantels of dark clouds in cold, quiescent regions. Even the detection limit estimated for crystalline ice (in the few per thousand) is probably too high. In practice, many observational lines of sight integrate ice signals from different temperature regions with variable proportions of crystalline and amorphous ice. The analysis is therefore complex, and the estimate of the HDO/H_2O solid state ratio in astronomical environments by IR spectroscopy may have limited value.

In Figure 3, we show the results of H/D exchange in ice layers initially deposited at 14 K, 90 K, and 150 K from a vapor mixture with a D_2O/H_2O ratio of 0.4%. The deposition conditions correspond, respectively, to microporous amorphous ice, compact amorphous ice, and crystalline (cubic) ice (Baragiola 2003). After deposition, the two first samples were heated to 150 K at a rate of 5 K minute^{-1}. Once the ice films had reached 150 K (time zero in Figure 3), isotopic

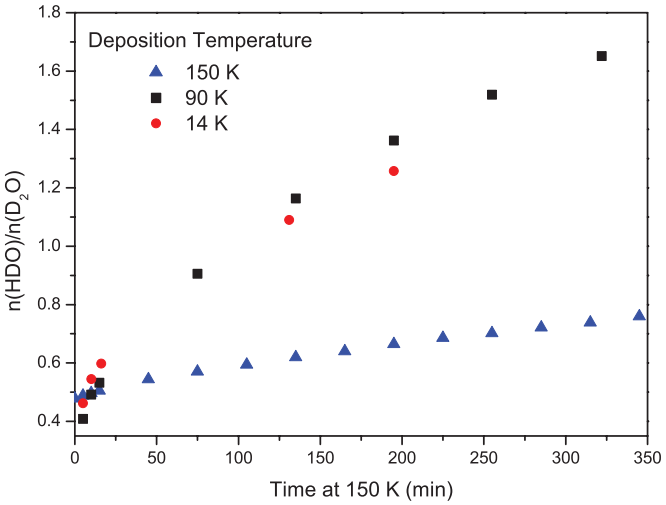

Figure 3. Evolution of the proportion of HDO with time for various HDO/H_2O ice samples at 150 K. All samples were produced by vapor deposition and the proportion of D_2O in the deposition vapor was 0.4%. Red dots: sample deposited at 14 K and heated to 150 K at 5 K minute^{-1}. Black squares: same for a deposition temperature of 90 K. Blue triangles: sample deposited directly at 150 K. The time origin for the annealed samples is taken when they first reach 150 K.

(A color version of this figure is available in the online journal.)

exchange was followed as a function of time by monitoring the quotient of the OD stretch band intensities in HDO and D_2O, respectively. At the beginning, the HDO/D_2O ratio was similar ($\sim$0.5) in all cases, but a divergence appeared with time between the films initially deposited in amorphous form and that directly produced with a crystalline structure. The samples deposited at 14 and 90 K evolved in a parallel way, with the amount of HDO equaling that of D_2O in about two hours and growing then further. In contrast, for the ice film deposited at 150 K isotopic exchange was found to be much slower and the HDO/D_2O quotient grew only to $\sim$0.7 after nearly six hours. After the same time, the ratio of HDO to D_2O had reached $\sim$1.7 for the film produced at 90 K. The higher rate of isotope exchange observed in the annealed samples strongly suggests that, in comparison with direct crystalline deposition, the annealing procedure leads to a higher proportion of defects in the crystalline ice being formed. Although the role of the ice surface in the creation and propagation of defects to the bulk material is still debated (Devlin & Buch 2007; Lee et al. 2006) it is likely that a different polycrystalline morphology with a surface to volume ratio more favorable for defect activity is formed in the annealed samples. On the other hand, the similarity in the evolution of the samples initially deposited as amorphous ice at 14 and 90 K indicates that the collapse of the microporous structure induced upon heating from 14 to 90 K (Raut et al. 2007; Herrero et al. 2010) produces a similar morphology to that obtained by direct deposition at 90 K.

The enhanced H/D exchange rate observed in the transition from the amorphous to the crystalline structure is consistent with the recent results of Ratajczak et al. (2009) who reported an appreciable depletion of the hydroxilic D in mixtures of deuterated methanol with H_2O for $T > 120$ K, and with the previous data of Kawanowa et al. (2004), who found also isotopic exchange at the hydroxylic group in mixtures of CH_3OH:D_2O at 140 K.

We have further investigated the transformation of D_2O in HDO by changing the initial D_2O/H_2O proportion. The results are shown in Figures 4 and 5. The three left panels of Figure 4 display the evolution with time of the IR spectra of ice layers

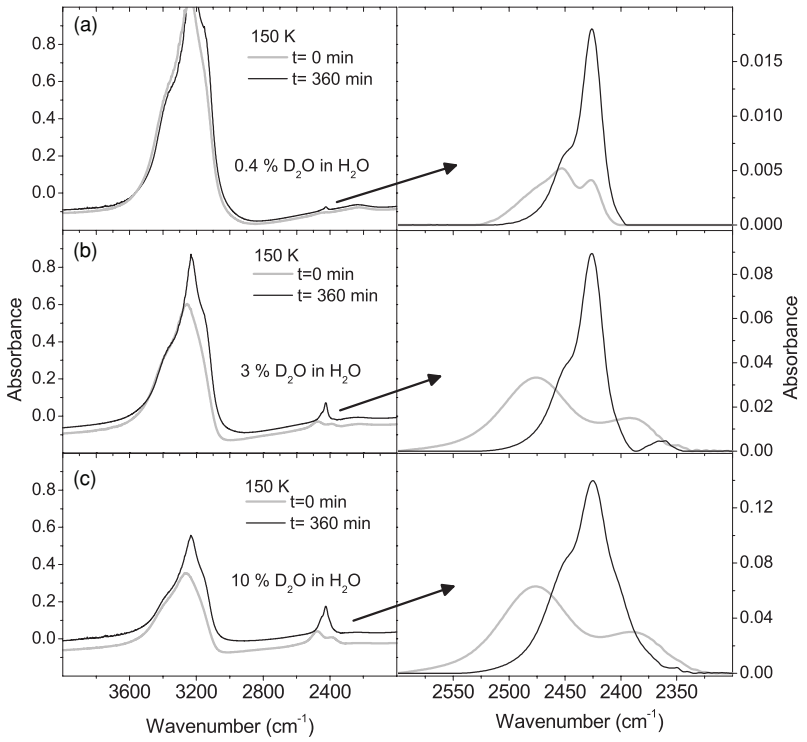

Figure 4. IR spectra of D_2O:H_2O mixtures generated at 90 K and heated to 150 K at 5 K minute^{-1}. The spectra were recorded when the ice samples first reached 150 K ($t = 0$) and 360 minutes afterward. Left panels (a), (b), and (c) correspond to D_2O mixture proportions of 0.004, 0.03, and 0.1, respectively. The corresponding right panels show an enlargement of the OD stretching region.

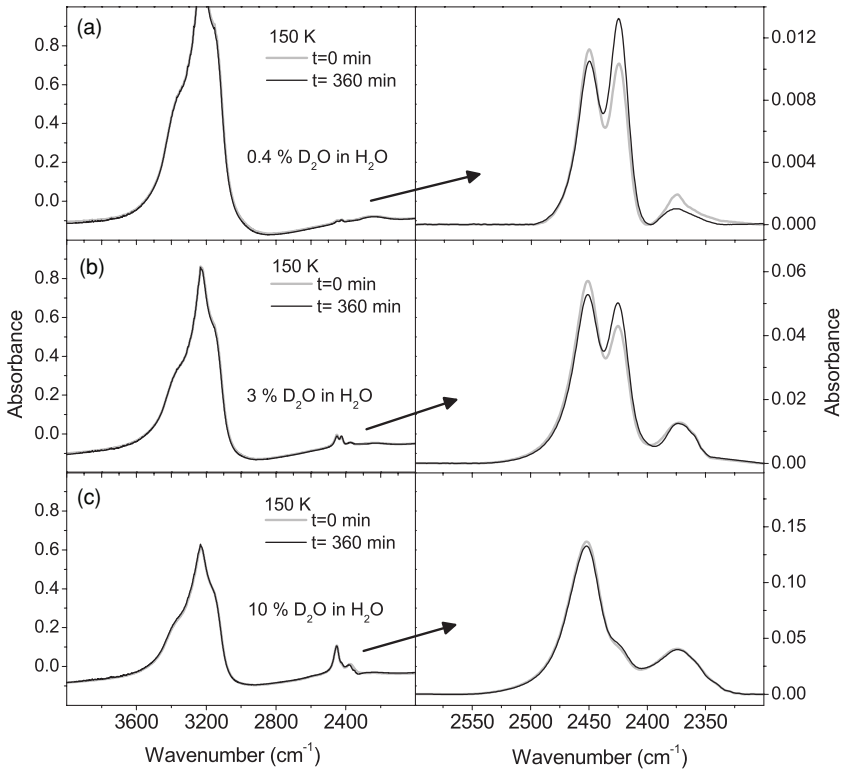

Figure 5. Same as Figure 4, but for crystalline ice, directly generated by deposition at 150 K.

initially deposited at 90 K and then warmed up to 150 K. The spectra, corresponding to D_2O/H_2O ratios of 0.4%, 3%, and 10%, are represented over the 4000–2000 cm^{-1} range and, as in Figure 3, time zero is counted when the layer first reaches a temperature of 150 K. Although the OH stretching band of H_2O at about 3200 cm^{-1} displays already the characteristic traits of a crystalline ice structure at $t = 0$, the band shape evolves further in the course of the experiment showing that the full molecular rearrangement during crystallization is relatively slow. The three right panels of the same figure show an enlargement of the OD region and illustrate the D_2O to HDO conversion in the various samples. The spectra at $t = 0$ exhibit two relatively broad bands.

The higher frequency band corresponds to the antisymmetric stretching of D_2O and the lower frequency band to the OD stretching of HDO; the weaker OD symmetric stretching band of D_2O at lower frequencies is poorly appreciable. In all cases, after 360 minutes the two bands become narrower, and blend appreciably, and the proportion of HDO with respect to D_2O increases. Note however that the larger D_2O to HDO conversion corresponds to the sample less concentrated in D_2O. Figure 5 shows the results of analogous experiments carried out for ice films with the same D_2O proportions, but directly deposited in the crystalline phase. The higher degree of ordering of these samples is immediately obvious from the better resolved spectral peaks. Now, the weaker OD symmetric stretch band of D_2O is clearly visible at lower frequencies in the enlarged spectra. As expected from the previous discussion of Figure 3, isotopic exchange is much lower than that observed in the corresponding annealed samples and is larger for the higher dilution (upper panel). In fact, in the sample with the highest D concentration (lower panel), virtually no change is observed after 350 minutes at 150 K. The combined results of Figures 4 and 5 suggest that above a certain (small) D proportion, isotopic H/D exchange in ice samples is not limited by the availability of D atoms, but rather by the relative amount of defects in the ice network, which is expected to be larger in the more disordered films crystallizing through annealing from amorphous samples and should be essentially independent of the isotopic composition of the ice. It should be noted that in the two samples with a 0.1 D_2O/H_2O ratio of Figures 3 and 4, the formation of some D_2O clusters might also limit the proton exchange process.

4. CONCLUSIONS

The sensitivity of IR spectroscopy for the detection of HDO in astronomical ice is strongly dependent on ice structure. The OD stretch band in the ~2400–2500 cm^{-1} range is usually employed for HDO detection, but, due to the large local disorder, this band becomes extremely broad and tends to disappear into the absorption continuum of H_2O in amorphous samples. The present measurements suggest that HDO/H_2O ratios smaller than a few percent are undetectable in low-temperature amorphous ice. On the other hand the narrowing of the band observed with growing temperature would allow, in principle, the detection of HDO in more ordered crystalline ice in a proportion as low as a few per thousand. This difference of an order of magnitude in sensitivity can pose a serious difficulty for the evaluation of HDO IR absorption measurements toward protostars, since the lines of sight can include variable proportions of amorphous and crystalline ice. It seems that in spite of some technical difficulties gas-phase millimeter wave techniques can provide better estimates or the HDO/H_2O ratio in protostellar environments (Jørgensen & van Dishoeck 2010).

Isotopic H/D exchange in mixed ice of H_2O/D_2O is found to start at temperatures beyond ~120 K and to accelerate greatly at ~150 K, in accordance with previous observations. The rate of exchange, which can be followed by monitoring the evolution of the OD band of HDO, depends on the procedure of ice formation. Annealed amorphous samples are more favorable for isotope exchange than samples directly deposited in the crystalline phase. In accordance with the accepted mechanism, which assumes that isotope exchange is brought about by the propagation of charge and orientational defects in ice, the annealing of amorphous ice samples seems to provide a polycrystalline morphology with a higher defect activity. Additional experiments suggest that, except for high isotopic dilutions, defect activity might be the limiting step in isotopic exchange. These results support the view that solid state reactions, and not just previous gas-phase ion-molecule chemistry, can affect the isotopic fractionation observed in hot core molecules evaporating from grain mantels. In particular the present data emphasize the relevance of a depletion mechanism for D atoms in hydroxylic bonds in the solid state, recently advanced by Ratajczak et al. (2009) that could contribute to explaining the low relative abundance of the CH_3OD isotopomer in protostellar sources.

This research has been funded by the MCINN of Spain under grants FIS2007-61686 and FIS2010-16455. O.G. acknowledges funding from "Ramón y Cajal" program. We thank M. A. Moreno for technical support. We are also indebted to the anonymous referee who provided valuable suggestions for the improvement of this article.

REFERENCES

Baragiola, R. A. 2003, Planet. Space Sci., 51, 953
Bockelée-Morvan, D., Gautier, D., Lis, D. C., et al. 1998, Icarus, 133, 147
Carrasco, E., Castillo, J. M., Escribano, R., et al. 2002, Rev. Sci. Instrum., 73, 3469
Ceccarelli, C., Caselli, P., Herbst, E., Tielens, A. G. G. M., & Caux, E. 2007, in Protostars and Planets V, ed. B. Reipurth, D. Jewitt, & K. Keil (Tucson, AZ: Univ. Arizona Press), 47
Collier, W. B., Ritzhaupt, G., & Devlin, J. P. 1984, J. Phys. Chem., 88, 363
Dartois, E., Thi, W.-F., Geballe, T. R., et al. 2003, A&A, 399, 1009
Devlin, J. P. 1990, Int. Rev. Phys. Chem., 9, 29
Devlin, J. P., & Buch, V. 2007, J. Chem. Phys., 127, 091101
Gálvez, O., Maté, B., Herrero, V. J., & Escribano, R. 2008, Icarus, 197, 599
Geil, B., Kirschgen, T. M., & Fujara, F. 2005, Phys. Rev. B, 72, 014304
Herrero, V. J., Gálvez, O., Mate, B., & Escribano, R. 2010, Phys. Chem. Chem. Phys., 12, 3164
Hague, W., Hallbrucker, A., Mayer, E., & Johari, P. 1994, J. Chem. Phys., 100, 2743
Ikawa, S. I., & Maeda, S. 1968, Spectrochim. Acta A, 24, 665
Jørgensen, J. K., & van Dishoeck, E. 2010, ApJ, 725, L172
Kawanowa, H., Kondon, M., Gotho, Y., & Souda, R. 2004, Surf. Sci., 566, 1190
Kouchi, A., & Yamamoto, T. 1995, Prog. Cryst. Growth Charact., 30, 83
Lee, C. W., Lee, P. R., & Kang, H. 2006, Angew. Chem. Int. Ed., 45, 5529
Lee, C. W., Lee, P. R., Kim, Y. K., & Kang, H. 2007, J. Chem. Phys., 127, 084701
Liu, F. C., Parise, B., Kristensen, L., et al. 2011, A&A, 527, A19
Loinard, L., Castets, A., Ceccarelli, C., et al. 2002, Planet. Space Sci., 50, 1205
Madden, W. G., Bergren, M. S., McGraw, R., Rice, S. A., & Sceats, M. G. 1978, J. Chem. Phys., 69, 3497
Mastrapa, R. M., Sandford, M. A., Roush, T. L., Cruikshank, D. P., & Dalle Ore, C. M. 2009, ApJ, 701, 1347
Maté, B., Medialdea, A., Moreno, M. A., Escribano, R., & Herrero, V. J. 2003, J. Phys. Chem. B, 107, 11098
Mayer, E., & Pletzer, M. 1985, J. Chem. Phys., 83, 6536
Millar, T. D. 2005, Astron. Geophys., 46, 2.29
Palumbo, M. E. 2005, J. Phys.: Conf. Ser., 6, 211
Parise, B., Castets, A., Herbst, E., et al. 2004, A&A, 416, 159
Parise, B., Caux, E., Castets, A., et al. 2005, A&A, 431, 547
Parise, B., Simon, T., Caux, E., et al. 2003, A&A, 410, 897
Ratajczak, A., Quirico, E., Faure, A., Schmitt, B., & Ceccarelli, C. 2009, A&A, 496, L21
Raut, U., Famá, M., Loeffler, M. J., & Baragiola, R. A. 2008, ApJ, 687, 1070
Raut, U., Famá, M., Teolis, B. D., & Baragiola, R. A. 2007, J. Chem. Phys., 127, 204713
Robert, F. 2001, Science, 293, 1056
Robert, F., Gautier, D., & Dubrulle, B. 2000, Space Sci. Rev., 92, 201
Roberts, H., Herbst, E., & Millar, T. J. 2002, MNRAS, 336, 283
Rodgers, S. D., & Millar, T. J. 1996, MNRAS, 280, 1046
Stark, R., Sandell, G., Beck, S. C., et al. 2004, ApJ, 608, 341
Teixeira, T. C., Devlin, J. P., Buch, V., & Emerson, J. P. 1999, A&A, 347, L19
Tielens, A. G. G. M. 1983, A&A, 119, 177
Turner, B. E. 2001, ApJS, 136, 579
Villanueva, G. L., Mumma, M. J., Bonev, B. P., et al. 2009, ApJ, 690, L5
Watanabe, N., & Kouchi, A. 2008, Prog. Surf. Sci., 83, 439